Available online at www.sciencedirect.com
ScienceDirect
Trans. Nonferrous Met. Soc. China 34(2024) 2260−2274
Transactions of Nonferrous Metals Society of China
www.tnmsc.cn

Oxidation behavior of Cu-based brake pad for high-speed train

Jin-kun XIAO[1], Tian-tian LI[1], Ting-feng BAO[1], Juan CHEN[2], Chao ZHANG[1]

1. School of Mechanical Engineering, Yangzhou University, Yangzhou 225127, China;
2. Testing Center, Yangzhou University, Yangzhou 225009, China

Received 4 January 2023; accepted 20 July 2023

Abstract: Cu-based brake pad for high-speed train undergoes cyclic oxidation due to the generation and dissipation of friction heat during braking. The oxidation behavior of the Cu-based brake pad was investigated via isothermal oxidation at 300, 400, 500, 600 and 700 °C for up to 50 h. The results show that the oxidation of the Cu-based brake pad presents multiple stages. The combination of the oxidation of Cu and Fe and the oxygen diffusion controls the oxidation process in the earlier stage, while the oxidation of graphite plays a more important role in the later stages above 500 °C. The Cu_2O nanoclusters are firstly formed by the oxidation of copper, then CuO nanowires, and finally fine and coarse equiaxed grains are generated. The rise in temperature promotes the growth and densification of Fe_2O_3 nanosheets, which grow on the Fe_3O_4 layer. However, Fe oxides are gradually covered by Cu oxides because of the larger volume expansion of Cu oxides. The connected pores formed by the graphite burn-off provide oxygen diffusion channels for internal oxidation. The improved surface microhardness is attributed to the formation of oxides.
Key words: Cu-based brake pad; isothermal oxidation kinetics; oxidation behavior; surface morphology

1 Introduction

China's Fuxing high-speed train (Fig. 1(a)) today has broken numerous world records in addressing challenging speed, climate and environmental conditions [1−3]. Braking pads for high-speed trains require stable friction coefficient, high wear resistance, good thermo-mechanical properties, low mating disc wear and excellent adaptability [4−7]. They have to be operated at a high temperature (>500 °C) for a long duration (>100 s) without failure or extensive wear. Cu-based friction composites are the leading brake pads because of their high thermal conductivity, low wear rate, and good matching properties [8−12]. These advantages are unfortunately coupled with low softening and oxidation temperatures, which severely restrict the operating temperature and application range. With the development of high-speed trains towards higher speed and heavier load, high temperature caused by emergency braking is a critical concern for the Cu-based brake pads.

The main function of friction materials is to convert kinetic energy into friction heat. The absorbing energy and maximum temperature of brake pad in high-speed trains rise gradually with increasing the braking speeds [4−19], as shown in Figs. 1(b, c). ZHANG et al [16] simulated the continuous emergency braking of Cu-based brake pad at 350 km/h and found that instantaneous surface temperature exceeded 900 °C. Phenomena of oxidation, softening and thermal fatigue occurred in brake pads at high temperature, which also led to the degradation of braking performance and the aggravation of wear [17,18]. In fact, the tribological

Corresponding author: Jin-kun XIAO, Tel: +86-15195562127, E-mail: jkxiao@yzu.edu.cn;
Chao ZHANG, Tel: +86-514-87971980, E-mail: zhangc@yzu.edu.cn
DOI: 10.1016/S1003-6326(24)66539-8

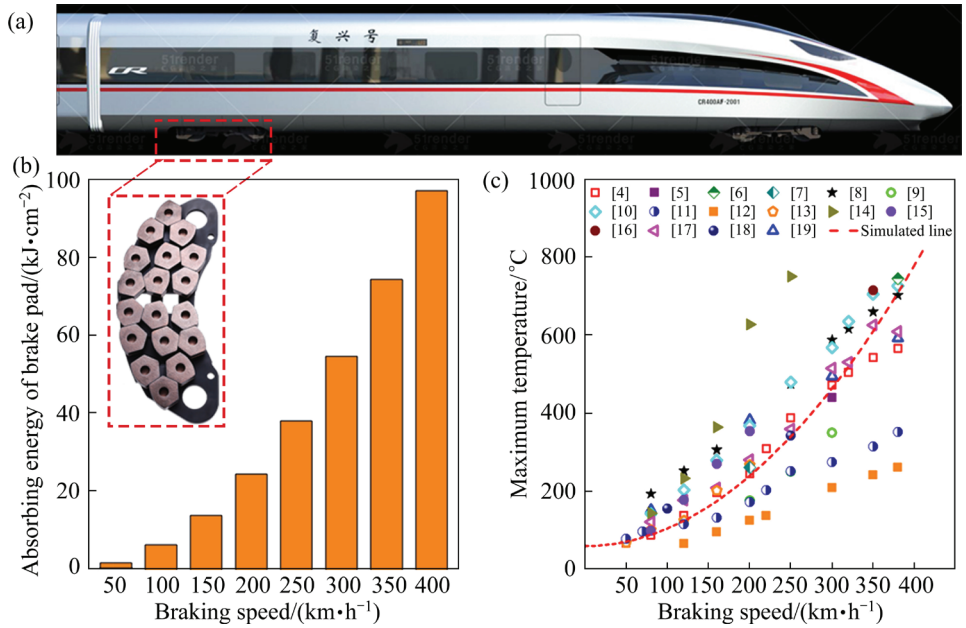

Fig. 1 Fuxing high-speed train (a); Absorbing energy of brake pad versus braking speed (b) and maximum temperature versus braking speed (c) for Cu-based brake pads

properties of Cu-based brake pads depend not only on the matrix, but also on the friction-induced oxide layer. The content of metal components in brake pads ranges from 60 to 80 wt.%, and the generated oxides are mainly copper and iron oxides. PENG et al [19] found that the tribolayer of Cu-based brake pads was mainly composed of metal (Cu, Fe) and oxides (FeO, Cu_2O and CuO). FeO would be further oxidized to the Fe_3O_4 and Fe_2O_3 at higher friction temperature. JAYASHREE et al [20] reported that the tribolayer was mainly composed of compacted CuO/Cu_2O oxides and iron oxides (mainly Fe_3O_4) transferred from the mating disc. STADLER et al [21] observed 10−15 nm oxide layer with a double-layer structure composed of CuO and Fe_2O_3 on the surface of metal-based brake pads. Hence, investigating the oxidation behavior of metal components in Cu-based brake pads is one of the most fundamental requirements to understand the formation of tribolayer.

Graphite is one of the most important lubricating components in Cu-based brake pads. However, its oxidation resistance is poor. When the temperature exceeds 400 °C, graphite will react with the oxygen and generate CO_2. The oxidation rate will increase rapidly when the temperature is above 500 °C [22,23]. ZHANG et al [24] found that the graphite on the friction surface of Cu-based brake pads disappeared due to serious oxidation at 800 °C. In addition, the loss of graphite lubrication at the friction surface led to severe wear and an unstable friction coefficient. XIAO et al [25] observed many uniformly-distributed pores in the side of the Cu-based brake pad after braking at 380 km/h, which were created due to the graphite ablation. Oxidation also limits the application of C/C composites for high-speed trains. The C/C composites will be oxidized at high temperature and their mechanical properties decrease rapidly [26]. Therefore, the protective coatings have to be prepared to restrain the oxygen penetration and improve the oxidation resistance [27−30]. Thus, graphite has an inherent drawback of poor thermal stability in atmosphere condition, resulting in the loss of lubricating film at high temperatures.

It is recognized that oxidation can significantly change the composition and microstructure of the friction surface of Cu-based brake pads, so it is of great significance to investigate their oxidation properties at high temperatures. In this work, the oxidation behavior of Cu-based brake pads was investigated by isothermal oxidation tests and thermo-gravimetric analysis. The oxidation kinetics of brake pads was analyzed, and the composition, microstructure and mechanical properties of the oxide films were examined. The related oxidation mechanism was also discussed.

2 Experimental

2.1 Materials

Cu-based brake pads for high-speed train in this study were synthesized by powder metallurgy method. Powders of electrolytic Cu (99.5% in purity, <75 μm), reduced Fe (99% in purity, <75 μm), CrFe alloy (95% in purity, <250 μm), flake graphite (95% in purity, <500 μm), MoS_2 (96% in purity, <6.5 μm), SiC (99% in purity, <38 μm) and others with a composition listed in Table 1 were used as starting materials. The powders was firstly mixed in a V-cone blender for 8 h, and then cold pressed at 400 MPa in a steel die to get hexagonal green compacts. The green compacts were subsequently placed on copper-plated steel backings, and then sintered at 950 °C under a pressure of 3 MPa for 2 h in an N_2+H_2 atmosphere in Bell furnace. After sintering, the samples were cooled down to room temperature in the furnace. Figure 2 shows optical images of the prepared Cu-based brake pad. The oxidation test samples of 10 mm × 10 mm × 10 mm in dimension were sectioned from the Cu-based brake pad.

Table 1 Composition of Cu-based brake pad (wt.%)

Cu	Fe	CrFe	Graphite	MoS_2	SiC	Others
45−50	10−15	5−8	15−20	2−5	2−5	3−5

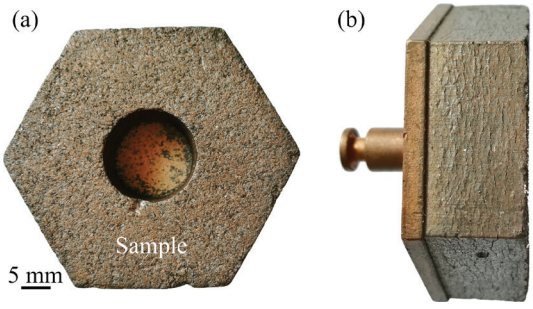

Fig. 2 Optical images of Cu-based brake pad: (a) Top view; (b) Side view

2.2 Oxidation tests

The oxidation behavior of the Cu-based brake pad samples was evaluated by isothermal oxidation tests. The samples were polished against 1500 grit SiC paper. Then, isothermal oxidation tests of samples were performed using an open-ended Al_2O_3 tube furnace (GSL−1700X, Hefei Kejing, China) in atmospheric condition at 300, 400, 500, 600 and 700 °C for 50 h, respectively. Once the furnace was heated to the target temperature, the samples were then pushed into the center of the furnace and held at the constant temperature for 5 h. After that, the samples were taken out from the furnace and air-cooled to the room temperature. The mass gains of samples were then measured using an analytical balance (BSA2202S, Sartorius, Germany) of 0.1 mg in accuracy. After weighing, the sample was put back into the furnace for a new round of oxidation test. This oxidation process was repeated for ten times at each temperature. Three independent samples were tested at each temperature in order to minimize experimental errors. The oxidized samples were called CBP300, CBP400, CBP500, CBP600 and CBP700, respectively.

In order to analysis the oxidation behavior of each component in the Cu-based brake pad, thermo-gravimetric analysis (TGA) of the main raw powders was conducted using an analyzer (Pyris 1 TGA, PerkinElmer, USA). The pure Cu, Fe and graphite powders were acquired directly from the raw materials. The Cu-based brake pad powder was filed from the sintered sample. The TGA tests were carried out at a heating rate of 10 °C/min from room temperature to 800 °C in flowing oxygen at 20 mL/min.

2.3 Characterization

The microstructure and chemical composition of oxidized samples were analyzed using a field-emission scanning electron microscopy (SEM, GeminiSEM 300, Zeiss, Germany) equipped with an energy-dispersive X-ray spectroscopy (EDS) detector. The crystal structure of the brake pad samples before and after oxidation was evaluated by X-ray diffraction (XRD, D8 Advance, Bruker, Germany) using a Cu K_α radiation at 40 mA and 40 kV. A 2θ scanning rate of 3 (°)/min and a distribution of 20°−80° were used during the tests. The oxidized surfaces was analyzed by X-ray photoelectron spectroscopy (XPS, Escalab 250Xi, Thermo Fisher Scientific, USA) using a mono-chromatic Al K_α X-ray excitation source. A wide scan survey and high-resolution spectrum were recorded. The microhardness of samples was measured using a microhardness tester (HV−1000, Huayin, China) with a load of 100 g and a dwell time of 15 s. The microhardness test of each sample was repeated ten times. The surface roughness of

oxidized samples was characterized by a 3D optical microscopy (ContourGT-K, Bruker, Germany).

3 Results and discussion

3.1 Microstructure of Cu-based brake pad

The typical microstructure of the Cu-based brake pad is presented in Fig. 3. In Fig. 3(a), the bright phase is the Cu component, the gray phase in the metal matrix is the Fe component, the light gray phase with the block shape is CrFe particle, and the dark phase is graphite. Elemental maps (Figs. 3(b−f)) reveal uniform distributions of Cu, Fe, Cr and C inside the composite. Besides, some SiC particles are also observed. The distribution regions of Cu, Fe and graphite phases do not overlap, indicating that the reaction and diffusion among these components are extremely limited during the sintering process. The three main components basically remain independent in the composite.

3.2 Oxidation behaviors of Cu-based brake pad

Figure 4 shows the isothermal oxidation curves of Cu-based brake pads oxidized at temperatures from 300 to 700 °C for 50 h. With the increase of oxidation time, the mass gain of the samples increases rapidly at first, and then increases gradually after reaching a critical mass. However, the mass gain of the samples does not simply show an increase tendency with increasing oxidation temperature. It decreases at 500 °C and then continues to increase. Cu-based brake pad is a multi-component composite, and its oxidation process is much more complicated than that of alloys. According to the main compositions, the isothermal oxidation of Cu-based brake pads can be simplified to the superposition of two kinds of oxidation processes. One is the oxidation mass gain of metal components (copper and iron), and the other is the oxidation mass loss of graphite. As shown in Fig. 4, there is an increase in the mass of

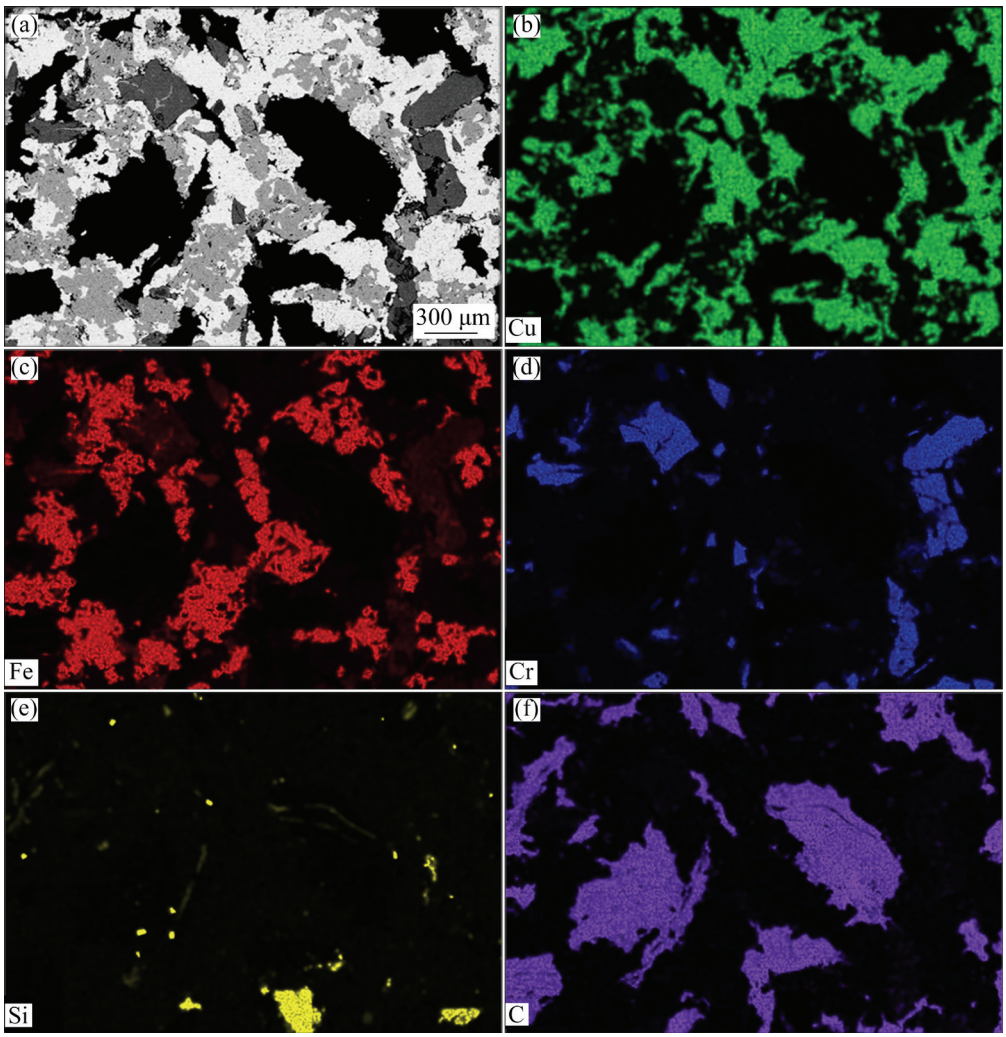

Fig. 3 Microstructure of Cu-based brake pad: (a) BSE image; (b−f) EDS maps

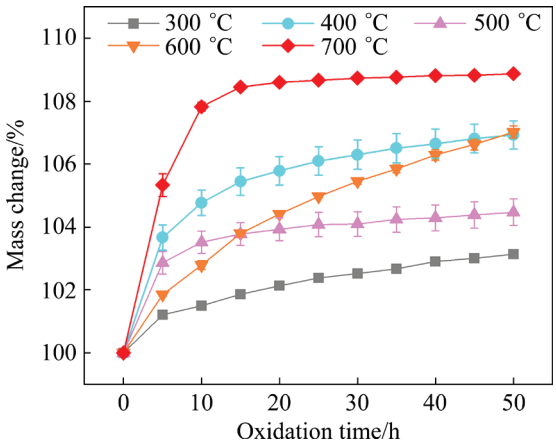

Fig. 4 Isothermal oxidation curves of Cu-based brake pad in air at temperatures from 300 to 700 °C

Cu-based brake pads with increasing oxidation time at each temperature. This means that the oxidation of Cu-based brake pads is going on, and the oxidation mass gain of metal components is greater than the ablation mass loss of the graphite.

In order to further investigate the oxidation behavior, thermo-gravimetric analysis of Cu-based brake pad and its main components (Cu, Fe and graphite powders) was carried out. Figure 5 shows the TGA and DTG (derivative thermo-gravimetric analysis) curves. The TGA curve shows the mass change of powder, while DTG curve shows the variation rate of the mass change curve. The Cu-based brake pad powder begins to gain mass at 300 °C and then loss mass at 665 °C. The mass gain rate decreases sharply at about 570 °C, indicating that the graphite begins to oxidize in large quantities at this temperature. The results in Fig. 5(d) further verify this. The graphite powder begins to burn off at 535 °C, and the mass decreases sharply. This is close to the oxidation temperature of graphite in brake pads [31,32]. Figure 5(b) presents the oxidation mass gain curve of Cu powder. The Cu powder begins to oxidize at 200 °C, and the oxidation rate increases with the temperature. However, the oxidation rate starts to decrease at 610 °C. The sharp decrease of oxidation rate may indicate that oxidation has entered the stage of diffusion control. The oxidation process of Fe powder is similar to that of Cu powder (Fig. 5(c)). Fe powder begins to oxidize at about 365 °C, and its oxidation rate increases until about 700 °C.

The Cu oxidation dominates at 300 °C. Due to the low temperature, the oxidation rate of Cu is low and the mass of brake pads increases slowly. At 400 °C, the oxidation of Cu accelerates and Fe

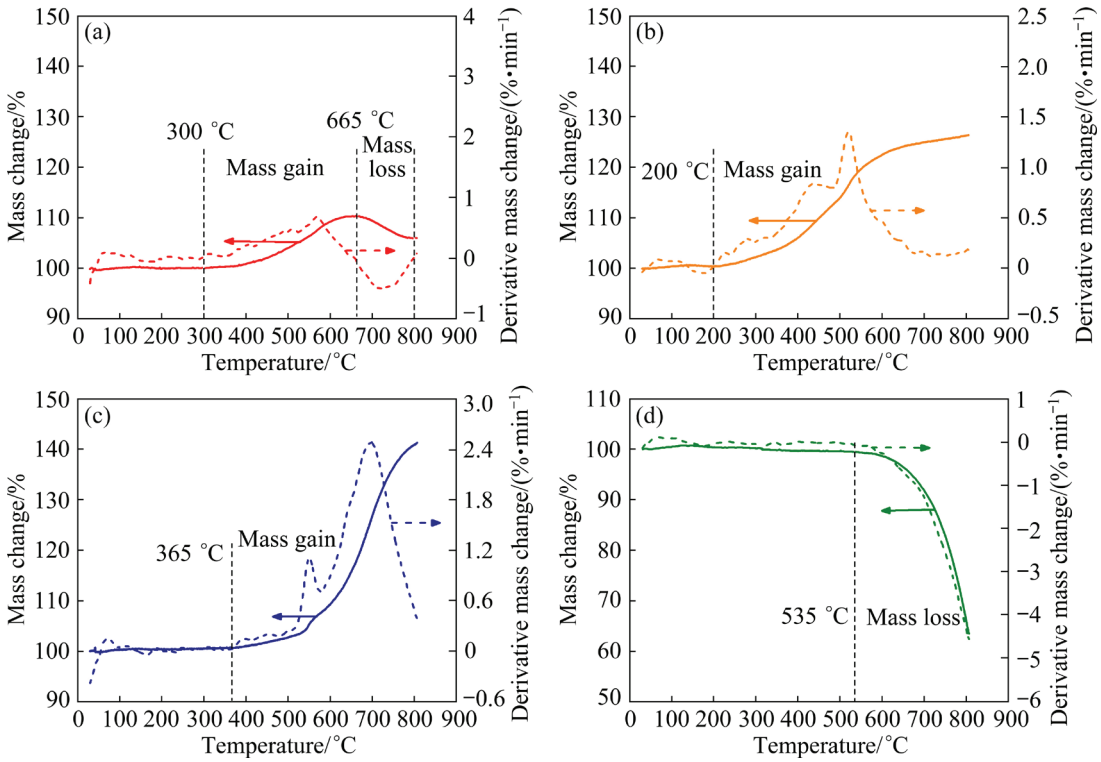

Fig. 5 TGA and DTG curves of Cu-based brake pad and its main components: (a) Cu-based brake pad powder; (b) Cu powder; (c) Fe powder; (d) Graphite powder

begins to oxidize. As a result, the oxidation mass gain of the brake pad is much higher than that at 300 °C. When the temperature is below 500 °C, the oxidation of graphite is in the stage of chemical control [22]. Its oxidation rate is very low and the oxidation mass loss can be ignored. At this time, the brake pads are mainly oxidized by metal matrix. However, the graphite oxidation begins to enter the stage of in-pore diffusion control above 500 °C [33,34]. The oxidation rate is high, and oxidation mass loss effect is significant with the increase of oxidation time. Although the oxidation of metal is further intensified at 500 °C, the mass gain of metal matrix is lower than the mass loss rate of graphite. Therefore, the mass gain of the brake pad at 500 °C is limited. The oxidation mass gain of brake pads increases with the further increase of temperature above 500 °C. This is related to the content and distribution of graphite in the composite. The mass ratio of graphite is only 15−20 wt.%, which is much lower than that of metal components (about 60 wt.%). Therefore, the change of total mass is limited when graphite is oxidized. In addition, the pores formed due to graphite oxidation are beneficial for oxygen to enter the interior of the sample. The oxidation area of the metal matrix is increased, and thus the oxidation mass gain is intensified.

3.3 Phase and morphology of Cu-based brake pad

Figure 6 shows the XRD patterns of Cu-based brake pads after the isothermal oxidation test at different temperatures. The XRD pattern of the original sample (25 °C) reveals that it is mainly composed of graphite and copper, and a small amount of Fe. Only Cu_2O is formed on the surface of Cu-based brake pad after the oxidation test at 300 °C, and the peak intensity of Cu declines greatly. This means that the Cu in the brake pad tends to be firstly oxidized to generate Cu_2O. The Cu_2O has a similar crystal structure (cubic system) to Cu, so Cu can be oxidized to Cu_2O without changing the topology structure. However, CuO has a monoclinic structure. Its formation needs to undergo complex process of atomic reconstruction, and the dynamic barrier is high. Therefore, the kinetic effect may be the decisive factor in the initial stage of oxidation, and Cu_2O is a more likely initial oxidation product of Cu [35−37]. At oxidation temperatures of 400 and 500 °C, both Cu_2O and CuO are formed on the surface of brake pad. In the meantime, the content of graphite declines and the Cu phase disappears. This illustrates that the brake pad undergoes more severe oxidation. The Cu_2O is converted to CuO, and the graphite begins to be oxidized. As the temperature rises to above 600 °C, the oxidation process is further aggravated. A large amount of CuO and a small amount of Fe_3O_4 and Fe_2O_3 are generated on the brake pad surface. Moreover, the graphite and Cu_2O phases disappear. With the increase of isothermal oxidation temperatures, the phases on the surface of copper-based brake pad change significantly. Therefore, the following reactions may occur:

$$2Cu(s)+1/2O_2(g)=Cu_2O(s) \quad (1)$$

$$Cu(s)+1/2O_2(g)=CuO(s) \quad (2)$$

$$Fe(s)+1/2O_2(g)=FeO(s) \quad (3)$$

$$3Fe(s)+2O_2(g)=Fe_3O_4(s) \quad (4)$$

$$2Fe(s)+3/2O_2(g)=Fe_2O_3(s) \quad (5)$$

$$C(s)+1/2O_2(g)=CO(g) \quad (6)$$

$$C(s)+O_2(g)=CO_2(g) \quad (7)$$

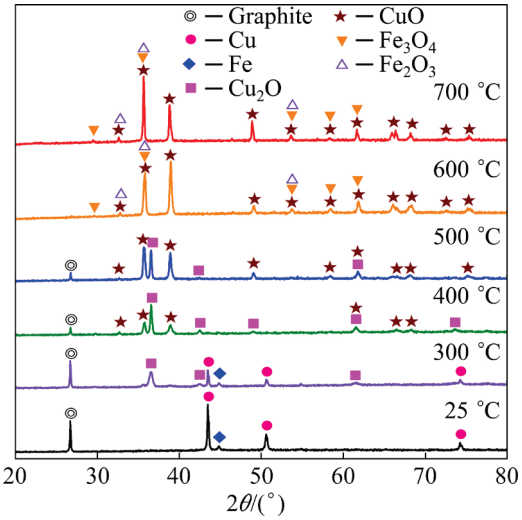

Fig. 6 XRD patterns of Cu-based brake pads oxidized at different temperatures

Figure 7 shows SEM images of the Cu-based brake pad oxidized at 300 °C. The CBP300 surface is covered with a discontinuous oxide film (Figs. 7(a, b)). The oxide film is composed of a large number of spherical oxide clusters (Fig. 7(c)), on which some short nanowires grow. According to

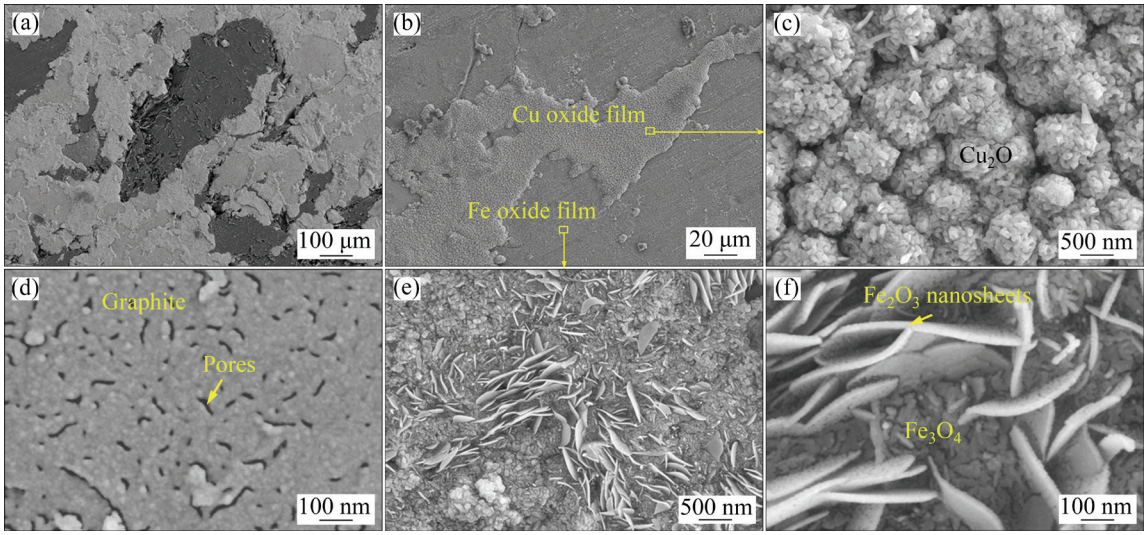

Fig. 7 SEM images of Cu-based brake pad oxidized at 300 °C: (a) Oxidized surface; (b) Oxidized metal matrix; (c) Cu oxide film; (d) Oxidized graphite; (e, f) Fe oxide film

the XRD results (Fig. 6), the oxide film is mainly Cu_2O, so it is covered on the surface of Cu components. As shown in Figs. 7(e, f), some nanosheet oxides were observed on the surface of Fe components. It is also shown that the surface is covered with coherent homogeneous oxide layer from which nanosheets grow. These nanosheets are randomly orientated. CUI et al [38] also found Fe_2O_3 with flaky morphology when studying the oxidation behavior of Fe-based eutectic materials at high temperature. According to the oxidation process, Fe will be oxidized into FeO, Fe_3O_4 and Fe_2O_3 in turn. The formation mechanism of sheet-like Fe_2O_3 can be explained by line defect diffusion of Fe in oxide layer. The Fe_2O_3 nanosheets nucleate firstly on the boundary of poroid Fe_3O_4. Then, the nucleus grows gradually to a sheet-like shape and the sheet-shaped crystal nucleus spreads to the surroundings until covering the whole surface of Fe_3O_4. Figure 7(d) shows the morphology of the oxidized graphite sheet. Nanoscale long strip pores are found on the surface of graphite crystals, which are formed by the preferential oxidation of active points.

Figure 8 shows the SEM images and EDS mappings of the Cu-based brake pad oxidized at 400 °C. Compared with the surface oxide film of CBP300, the oxide film of CBP400 is much rougher and thicker (Figs. 8(a, b)). As shown in Fig. 8(c), there are two regions with obvious differences in oxidation morphology on the CBP400 surface: thick oxide film and thin oxide film. A large number of nanowires grow on the thick oxide film, while many flaky oxides grow on the thin oxide film. According to EDS mappings (Figs. 8(g−i)), the above two morphologies correspond to the copper oxides and iron oxides, respectively. Combined with XRD results, these nanowires on the surface of CBP400 can be identified as CuO phase. The formation of CuO nanowires can be explained by the stress-induced growth model. In classical theory, the Cu matrix is firstly oxidized to form Cu_2O, and then the Cu_2O is further oxidized into CuO. The formation of oxides will introduce remarkable compressive strain inside the surface scale due to volume expansion, which can act as the driving force for the outward diffusion of Cu cations [39]. It was suggested that cumulative compressive stress could be generated at Cu/Cu_2O/CuO interface [40]. Grain boundary diffusion and rapid surface diffusion of Cu cations could be enabled under the action of the compressive stress. Therefore, Cu cations continuously diffuse outward to the nanowires root via grain boundaries driven by the compressive strain and feed the rapid growth of CuO monocrystal along special orientations. The sizes of pores on graphite (Fig. 8(d)) and flaky Fe_2O_3 (Fig. 8(f)) are much larger than those at 300 °C, indicating that oxidation gets enhanced with the temperature rising.

Figure 9 presents the SEM images of the Cu-based brake pad oxidized at 500 °C. The oxidation of the Cu-based brake pad is further intensified with

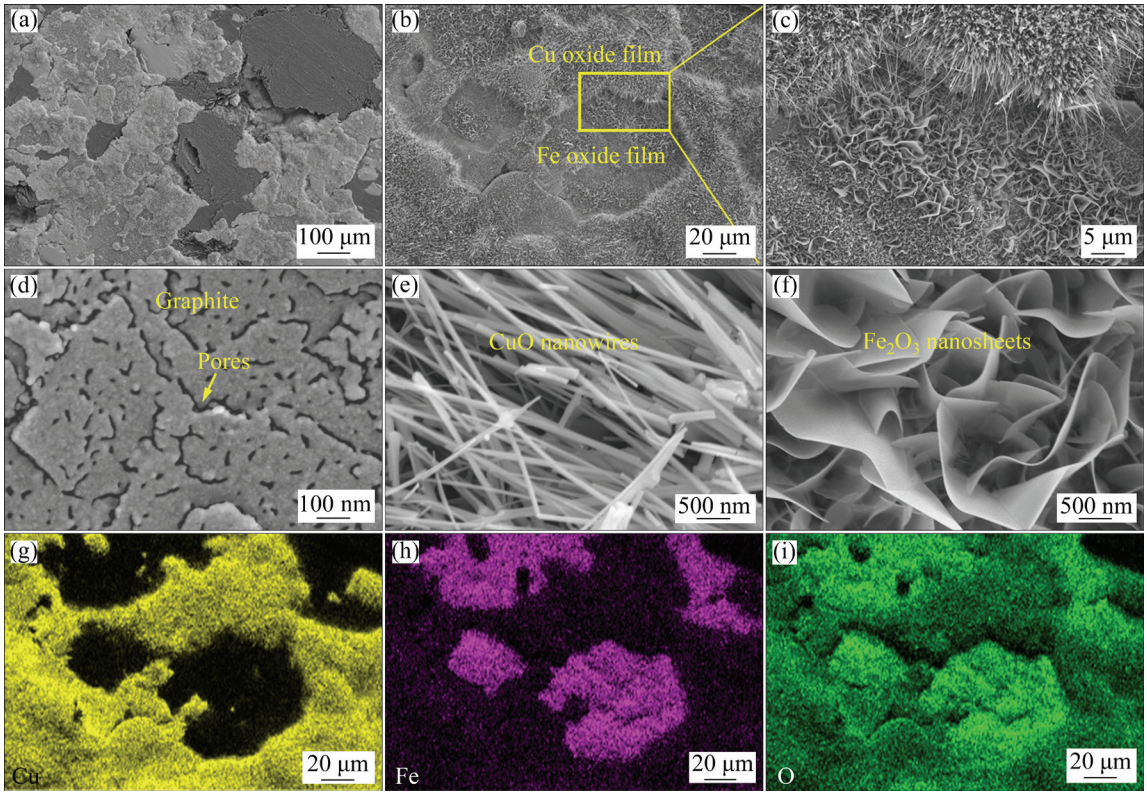

Fig. 8 SEM images and EDS mappings of Cu-based brake pad oxidized at 400 °C: (a) Oxidized surface; (b, c) Oxidized metal matrix; (d) Oxidized graphite; (e) CuO nanowires; (f) Fe_2O_3 nanosheets; (g−i) EDS maps of (b)

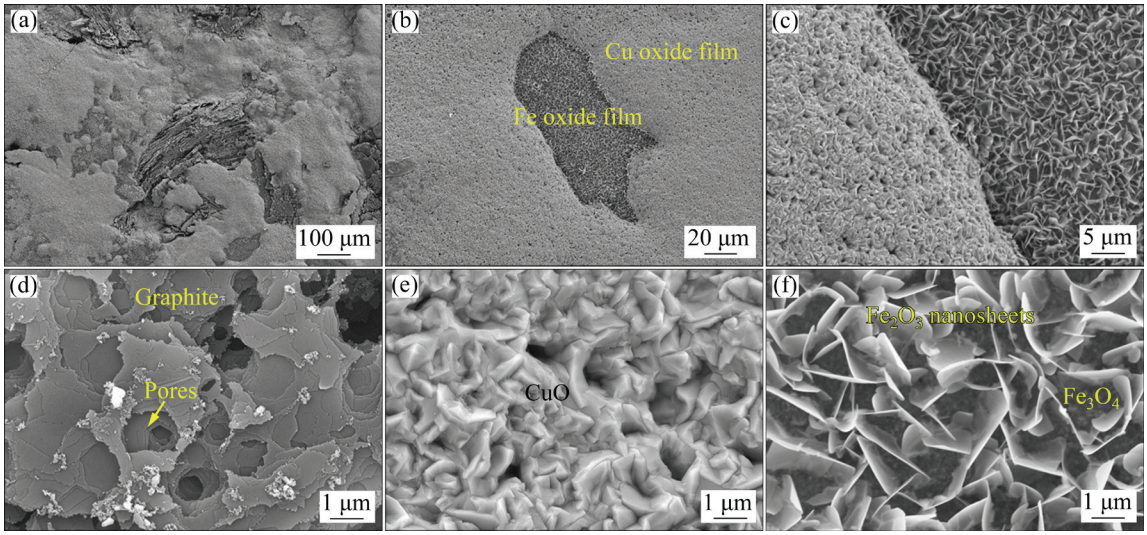

Fig. 9 SEM images of Cu-based brake pad oxidized at 500 °C: (a) Oxidized surface; (b, c) Oxidized metal matrix; (d) Oxidized graphite; (e) CuO grains; (f) Fe_2O_3 nanosheets

the increase of oxidation temperature. The CuO nanowires disappear and are replaced by CuO equiaxed grains (Figs. 9(c, e)). Fe_2O_3 nanosheets not only exist, but also get larger and denser, as shown in Fig. 9(f). The disappearance of CuO nanowires may be related to their special formation conditions. CAO et al [41] reported similar findings. CuO nanowires grow remarkably only in a temperature window of 400−700 °C. The absence of CuO nanowires below 400 °C is ascribed to insufficient copper diffusion at low temperature, while above 700 °C, "lattice diffusion" rather than "grain boundary diffusion" can result in the failure of CuO nanowires growth and lead to the growth of CuO nanograins. In addition, it should be noted that the coverage of Cu oxide film on surface increases,

while the coverage of Fe oxide film decreases. This is caused by the rapid growth rate and large volume expansion of Cu oxide film, which occupies the space of Fe oxide film. As shown in Fig. 9(d), many pores of ~1 μm are found in the graphite sheet, indicating that the oxidation ablation of graphite is very significant. As the temperature increases, the oxidation rates also increase, changing the microstructure of the graphite. The closed pores are opened and nanopores are converted to micropores to increase the reaction surface. The pores formed by oxidation on the graphite surface not only increase the reaction sites, but also provide more channels for oxygen diffusion.

The surface morphology of the Cu-based brake pad oxidized at 600 °C is displayed in Fig. 10. With further increase of the oxidation temperature, the chemical reaction rate accelerates greatly. Cracks are observed on the surface, which is caused by excessive internal stress in the thick oxide film. The graphite particles on the surface are burnt out, leaving a hollow net (Figs. 10(b, c)). This is consistent with the XRD results that the graphite peak nearly disappears. The grain size of CuO is obviously larger than that oxidized at 500 °C. Moreover, it can be seen from Figs. 10(a, d) that the Cu and Fe oxide films cannot be distinguished and the Fe_2O_3 nanosheets cannot be observed.

Figure 11 shows the SEM images and EDS mappings of the Cu-based brake pad oxidized at 700 °C. A large number of cracks and pores are created on the surface. All graphite particles on the surface of the brake pad are burned off, leaving big pores (Fig. 11(b)). In addition, the grain size of CuO reaches 5−10 μm. Figures 11(g−i) present the corresponding EDS mappings of Fig. 11(d). The sample surface is basically covered by copper oxide, while iron oxide exists only in a small part of the area. This is caused by the fast growth of Cu oxide film, which completely covers the surface of the sample including the Fe oxides area.

In order to determine the chemical composition of surfaces, the EDS analysis of Cu-based brake pads oxidized at 300 to 700 °C was carried out. The results are given in Table 2. With the increase in oxidation temperature, the content of Cu and O elements on the surface of brake pads increases; however, the content of Fe element shows a decreasing trend. The increase of O content indicates that the oxidation of the surface is intensified, while the increase of Cu content and the decrease of Fe content illustrate that the surface is gradually occupied by copper oxides. In addition, the decrease in C content further confirms the serious graphite burn-off at high temperatures.

The chemical states of oxidized surfaces at different temperatures analyzed by XPS are shown in Fig. 12. Elements of Cu, Fe, C and O are detected on the surfaces. In Fig. 12(a), the peaks of Cu $2p_{3/2}$ at 931.6, 932.7 and 933.6 eV represent Cu0 (pure Cu), Cu^{1+} (Cu_2O) and Cu^{2+} (CuO), respectively. The main peak of CBP300 is at 931.6 eV, indicating that there is less oxidation. With the increase of the temperature, the peak contribution at 932.7 and 933.6 eV is enhanced, indicating that Cu is oxidized. The Fe 2p spectra

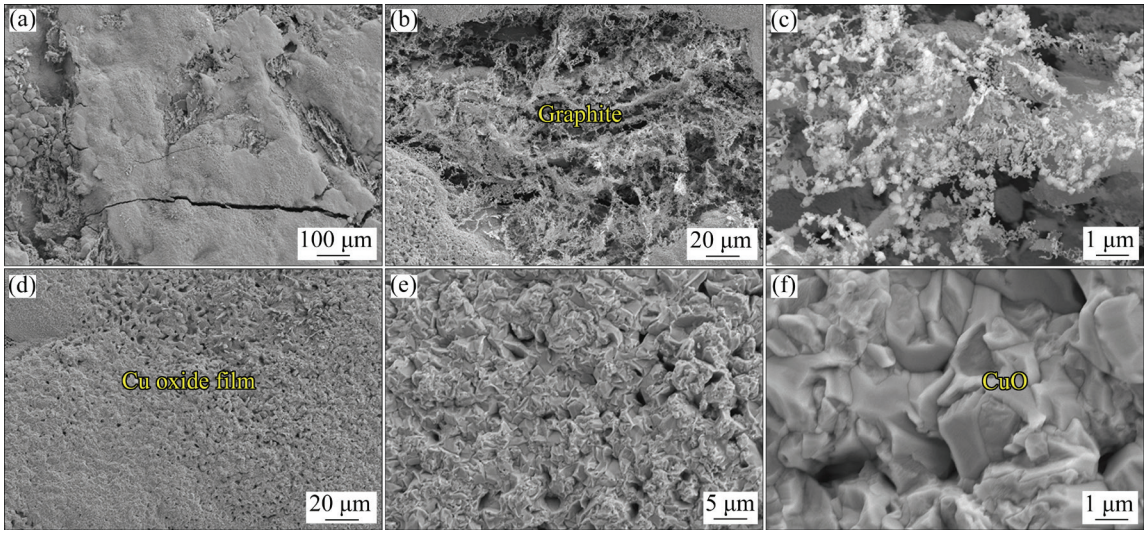

Fig. 10 SEM images of Cu-based brake pad oxidized at 600 °C: (a) Oxidized surface; (b, c) Oxidized graphite; (d) Cu oxide film; (e, f) CuO grains

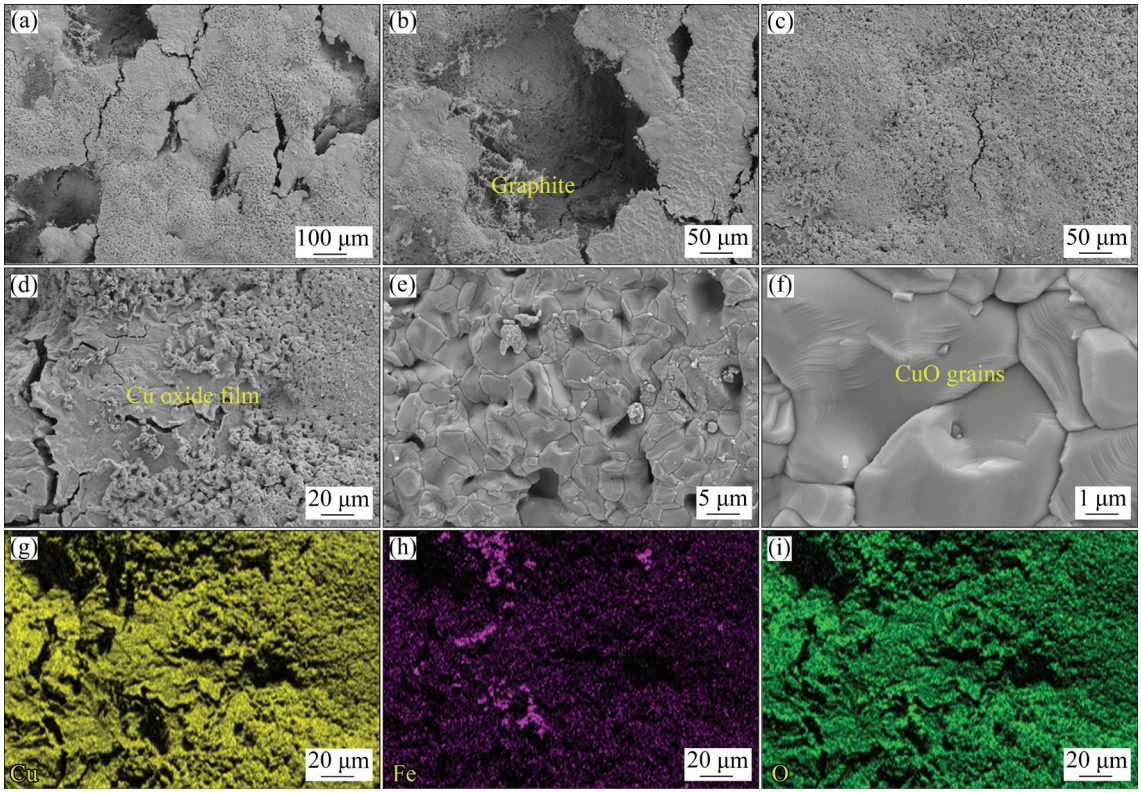

Fig. 11 SEM images and EDS mappings of Cu-based brake pad oxidized at 700 °C: (a) Oxidized surface; (b) Pore; (c) Oxidized metal matrix; (d) Cu oxide film; (e, f) CuO grains; (g−i) EDS maps of (d)

Table 2 EDS result of oxidized Cu-based brake pads (wt.%)

Sample	Cu	Fe	Cr	C	O
CBP300	40.59	19.78	2.81	23.3	13.52
CBP400	47.01	15.71	1.06	22.27	13.96
CBP500	53.26	14.14	1.41	15.99	15.20
CBP600	67.83	7.23	1.14	8.14	15.66
CBP700	72.16	3.65	0.52	7.87	15.80

obtained from the samples are shown in Fig. 12(b), demonstrating the coexistence of Fe^{2+} and Fe^{3+} (FeO, Fe_3O_4, and Fe_2O_3) [25,42]. In Fig. 12(c), the intensity of C peak decreases rapidly with the increase of oxidation temperature, which confirms the burn-off of graphite on the brake pad surface. The O 1s peak at 530.9 eV (OH^-) is related to the adsorption of water, while the peak at 529.2 eV (O^{2-}) is attributed to oxides (Fig. 12(d)). It is evident that a thick oxide film is formed on the surface of all samples except those oxidized at 300 °C.

Figure 13 shows the cross-sectional SEM images of Cu-based brake pads oxidized at different temperatures. The gray graphite is uniformly distributed in the bright metal matrix. With the increase in oxidation temperature, the number of pores near the sample surface increases gradually. Pores are formed due to the oxidation of graphite particles. Below 400 °C, graphite is only slightly oxidized and pores are very small (Figs. 13(a, b)). There is no obvious change in the microstructure of the brake pads. At 500 °C, graphite begins to oxidize and many pores are created around the sample (Fig. 13(c)). This indicates that the oxidation rate of graphite increases significantly. As the oxidation temperature increases to 600 and 700 °C, the graphite particles at the outermost of the samples are basically burned off, leaving a large number of pores (Figs. 13(d, e)). These pores cause a three-dimensional connected network to promote the internal oxidation of the samples. It is evident that only the core of the samples is not oxidized. Figure 13(f) shows the porosity of the samples. The porosity increases with the increase of oxidation temperature, and there is a jump at 500 °C. This means that the graphite begins to oxidize rapidly at this temperature.

The three-dimensional images of Cu-based brake pads after oxidation are shown in Fig. 14. As

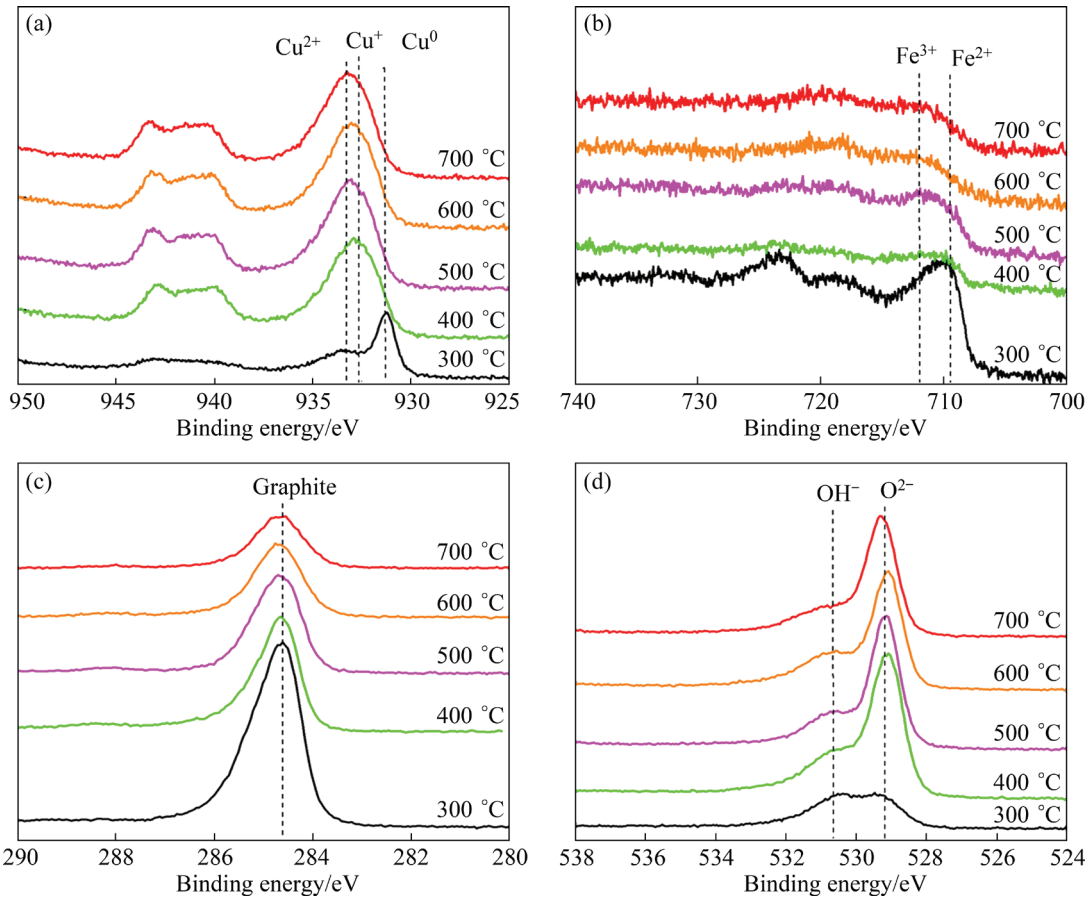

Fig. 12 XPS patterns of Cu-based brake pads oxidized at different temperatures: (a) Cu 2p; (b) Fe 2p; (c) C 1s; (d) O 1s

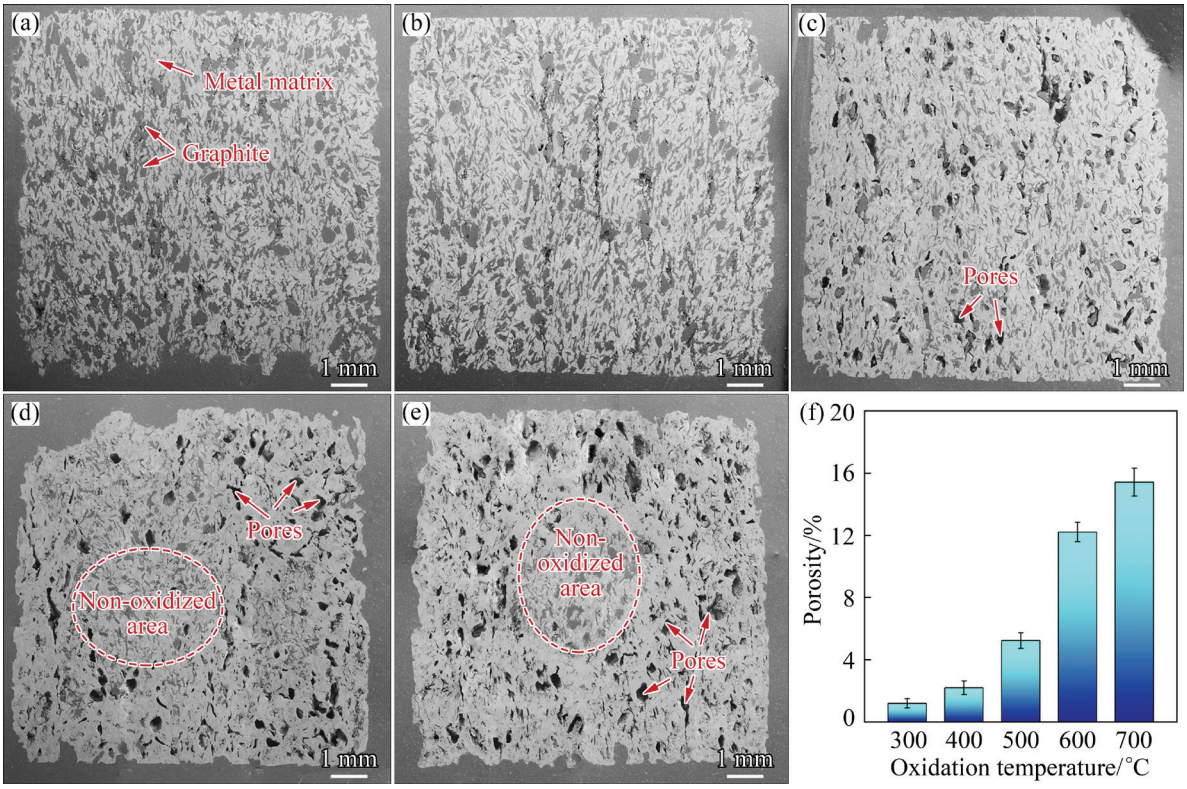

Fig. 13 Cross-sectional SEM images of Cu-based brake pads oxidized at different temperatures (a−e) and porosity (f): (a) 300 °C; (b) 400 °C; (c) 500 °C; (d) 600 °C; (e) 700 °C

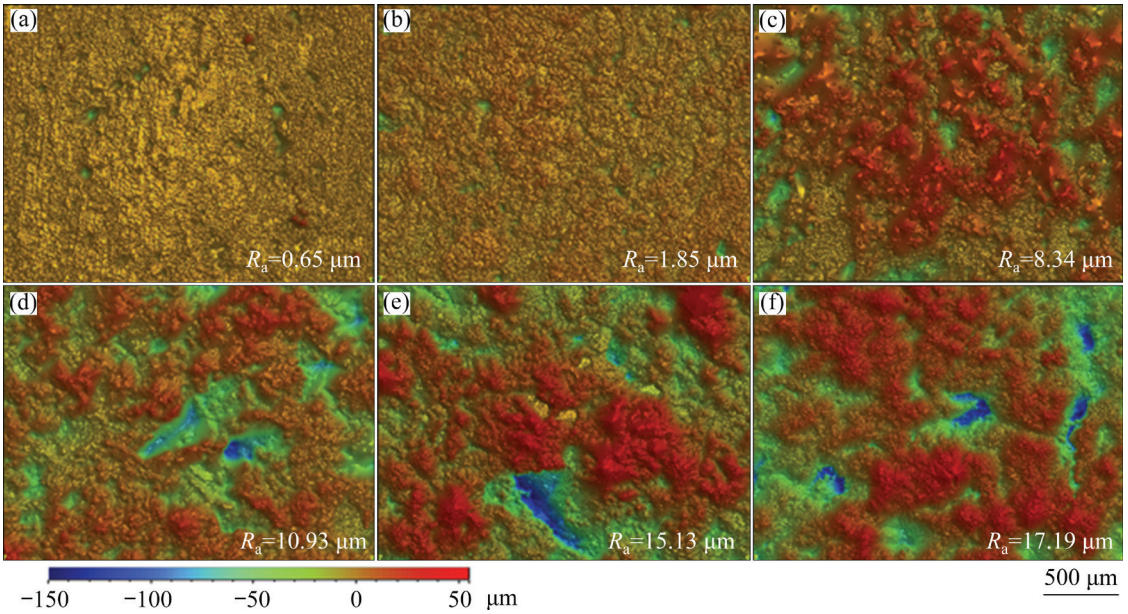

Fig. 14 Three-dimensional images of Cu-based brake pads oxidized at different temperatures: (a) 25 °C; (b) 300 °C; (c) 400 °C; (d) 500 °C; (e) 600 °C; (f) 700 °C

oxidation temperature increases from 25 to 700 °C, there is a corresponding rise in the surface roughness from 0.65 to 17.19 μm. Especially when the oxidation temperature is higher than 500 °C, there are many large and deep pores on the surface of the brake pad (Figs. 9(d−f)). As mentioned earlier, the formation of these pores is related to the oxidation of graphite. There are two reasons attributed to the increase of surface roughness. The oxidation of metal matrix (Cu and Fe) leads to the volume expansion and the formation of peaks. Besides, the oxidation of graphite particles results in the formation of pits.

Figure 15 shows the microhardness of Cu-based brake pads oxidized at different temperatures. The microhardness values of CBP25, CBP300, CBP400, CBP500, CBP600 and CBP700 are $HV_{0.1}$(101±16), $HV_{0.1}$(122±20), $HV_{0.1}$(188±32), $HV_{0.1}$(345±36), $HV_{0.1}$(365±38) and $HV_{0.1}$(307±40), respectively. The microhardness of the oxidized surface increases significantly with the increase of temperature and reaches the highest value at 600 °C. A large number of cracks on the surface result in the decrease of microhardness at 700 °C. Additionally, the microhardness of the oxidized brake pads is comparable to that of the tribolayer formed after high-energy braking, which is HV 250−350 [8,25]. The significant increase in microhardness is mainly caused by the formation of copper and iron oxides,

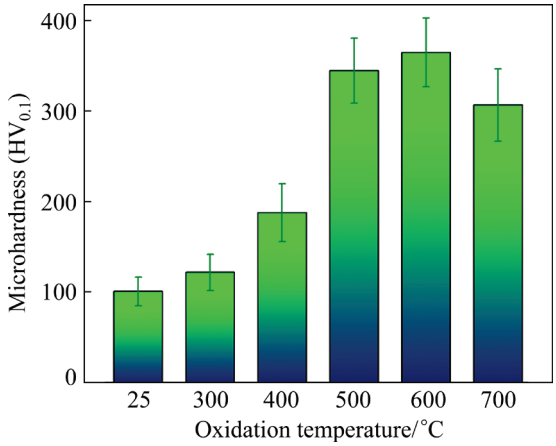

Fig. 15 Microhardness of Cu-based brake pads oxidized at different temperatures

which are believed to improve the wear of Cu-based brake pads [43].

4 Conclusions

(1) The oxidation of the Cu-based brake pad is carried out in multiple stages with the temperature increasing, because it is a multi-component composite. The initial oxidation sequence is Cu, Fe and graphite components. The combination of the oxidation of Cu and Fe and the oxygen diffusion controls the oxidation process in the earlier stage, while the oxidation of graphite plays a more important role in the later stages above 500 °C.

(2) The surface microstructure evolves significantly as temperature increases from 300 to 700 °C. The Cu_2O nanoclusters are firstly formed by the oxidation of copper, then CuO nanowires, and finally fine and coarse equiaxed grains are generated. The rise of temperature promotes the growth and densification of Fe_2O_3 nanosheets, which grow on the Fe_3O_4 layer. The volume expansion of Cu oxides is much larger than that of Fe oxides.

(3) The oxidation of graphite begins at the active sites and connects into lines below 500 °C, and the oxidation rate is very low. When the temperature is higher than 500 °C, the oxidation rate is very high and many large pores are formed. The connected pores provide a diffusion channel for oxygen, resulting in the internal oxidation of the Cu-based brake pad.

(4) The microhardness and surface roughness of Cu-based brake pads increase significantly with the increase of oxidation temperature. The improved mechanical property can be explained by the formation of the oxide film.

CRediT authorship contribution statement

Jin-kun XIAO: Conceptualization, Formal analysis, Funding acquisition, Investigation, Writing − Original draft, Writing − Review & editing; **Tian-tian LI:** Investigation, Methodology, Writing − Original draft; **Ting-feng BAO:** Investigation, Methodology; **Juan CHEN:** Investigation, Writing − Review & editing; **Chao ZHANG:** Resources, Writing − Review & editing.

Declaration of competing interest

The authors declare that they have no known competing financial interests or personal relationships that could have appeared to influence the work reported in this paper.

Acknowledgments

This work was supported by the National Natural Science Foundation of China (No. 51804272), High-end Talent Support Program of Yangzhou University (China), Qinglan Project of Yangzhou University (China), Yangzhou City−Yangzhou University Cooperation Foundation, China (No. YZ2022183), Postgraduate Research & Practice Innovation Program of Jiangsu Province, China (No. SJCX22_1716), and Innovation and Entrepreneurship Training Program for College Students of Jiangsu Province, China (No. 202211117173T).

References

[1] QI Yan-hui, ZHOU Li. The Fuxing: The China standard EMU [J]. Engineering, 2020, 6: 227−233.

[2] ZHAO Hong-wei, LIANG Jian-ying, LIU Chang-qing. High-speed EMUs: Characteristics of technological development and trends [J]. Engineering, 2020, 6: 234−244.

[3] WU Ying, LIU Yan, CHEN Hui, CHEN Yong, XIE Di. An investigation into the failure mechanism of severe abrasion of high-speed train brake discs on snowy days [J]. Engineering Failure Analysis, 2019, 101: 121−134.

[4] XIAO Ye-long, ZHANG Zhong-yi, YAO Ping-ping, FAN Kun-yang, Zhou Hai-bin, GONG Tai-min, ZHAO Lin, DENG Min-wen. Mechanical and tribological behaviors of copper metal matrix composites for brake pads used in high-speed trains [J]. Tribology International, 2018, 119: 585−592.

[5] WANG Zhi-zhong, HAN Jian-min, DOMBLESKY J P, LI Zhi-qiang, FAN Xin-guang, LIU Xiao-long. Crack propagation and microstructural transformation on the friction surface of a high-speed railway brake disc [J]. Wear, 2019, 428/429: 45−54.

[6] PENG Tao, YAN Qing-zhi, ZHANG Xiao-lu. Stability of metal matrix composite pads during high-speed braking [J]. Tribology Letters, 2018, 66: 63.

[7] MANN R, MAGNIER V, BRUNEL J F, DUFRENOY P, HENRION M, GUILLET-REVOL E. Thermomechanical characterization of high-speed train braking materials to improve models: Numerical validation via a comparison with an experimental braking test [J]. Tribology International, 2021, 156: 106818.

[8] ZHAO San-qing, YAN Qing-zhi, PENG Tao, ZHANG Xiao-lu, WEN Yu-ying. The braking behaviors of Cu-based powder metallurgy brake pads mated with C/C−SiC disk for high-speed train [J]. Wear, 2020, 448/449: 203237.

[9] ZHANG Peng, ZHANG Lin, FU Kang-xi, WU Pei-fang, CAO Jing-wu, SHIJIA Cai-rang, QU Xuan-hui. Effects of Ni-coated graphite flake on braking behavior of Cu-based brake pads applied in high-speed railway trains [J]. Journal of Tribology−Transactions of the ASME, 2019, 141: 081301.

[10] PENG Tao, YAN Qing-zhi, ZHANG Xiao-lu, ZHUANG Yan. Role of titanium carbide and alumina on the friction increment for Cu-based metallic brake pads under different initial braking speeds [J]. Friction, 2021, 9: 1543−1557.

[11] ZHANG Peng, ZHANG Lin, WEI Dong-bin, QU Xuan-hui. Effect of matrix alloying on braking performance of copper-based brake pad under continuous emergency braking [J]. Journal of Tribology−Transactions of the ASME, 2020, 142: 081703.

[12] ZHANG Peng, ZHANG Lin, FU Kang-xi, WU Pei-fang, CAO Jing-wu, SHIJIA Cai-rang, QU Xuan-hui. The effect of Al_2O_3 fiber additive on braking performance of copper-based brake pads utilized in high-speed railway train [J]. Tribology International, 2019, 135: 444−456.

[13] ZHAO San-qing, ZHANG Xiao-lu, ZHONG Wei-guang, WEN Yu-ying, YAN Qing-zhi. The wet braking and recovery behaviors of the P/M pad mated with C/C−SiC disc for

high-speed trains [J]. Wear, 2021, 468/469: 203609.

[14] SERRANO-MUNOZ I, RAPONTCHOMBO J, MAGNIER V, BRUNEL F, KOSSMAN S, DUFRÉNOY P. Evolution in microstructure and compression behaviour of a metallic sintered friction material after braking [J]. Wear, 2019, 436/437: 202947.

[15] XIAO Ye-long, YAO Ping-ping, ZHOU Hai-bin, ZHANG Zhong-yi, GONG Tai-min, ZHAO Lin, DENG Min-wen. Investigation on speed-load sensitivity to tribological properties of copper metal matrix composites for braking application [J]. Metals, 2020, 10: 889.

[16] ZHANG Peng, ZHANG Lin, FU Kang-xi, WU Pei-fang, CAO Jing-wu, SHIJIA Cai-rang, QU Xuan-hui. Fade behaviour of copper-based brake pad during cyclic emergency braking at high speed and overload condition [J]. Wear, 2019, 428/429: 10−23.

[17] PENG Tao, YAN Qing-zhi, LI Gen, ZHANG Xiao-lu, WEN Ze-feng, JIN Xue-song. The braking behaviors of Cu-based metallic brake pad for high-speed train under different initial braking speed [J]. Tribology Letters, 2017, 65: 135.

[18] ZHANG Xin, ZHANG Yong-zhen, DU San-ming, HE Tian-tian, YANG Zheng-hai. Influence of braking conditions on tribological performance of copper-based powder metallurgical braking material [J]. Journal of Materials Engineering and Performance, 2018, 27: 4473−4480.

[19] PENG Tao, YAN Qing-zhi, LI Gen, ZHANG Xiao-lu. The influence of Cu/Fe ratio on the tribological behavior of brake friction materials [J]. Tribology Letters, 2018, 66: 18.

[20] JAYASHREE P, BORTOLOTTI M, TURANI S, STRAFFELINI G. High-temperature tribo-oxidative wear of a Cu-based metal-matrix composite dry sliding against heat-treated steel [J]. Tribology Letters, 2019, 67: 110.

[21] STADLER Z, KRNEL K, KOVAC J, KOSMAC T. Tribochemical reactions on sliding surface of the sintered metallic brake linings against SiC ceramic brake disk [J]. Wear, 2012, 292/293: 232−238.

[22] LUO Xiao-wei, ROBIN J C, YU Su-yuan. Effect of temperature on graphite oxidation behavior [J]. Nuclear Engineering and Design, 2004, 227: 273−280.

[23] LUO Xiao-wei, ROBIN J C, YU Su-yuan. Comparison of oxidation behaviors of different grades of nuclear graphite [J]. Nuclear Engineering and Design, 2005, 151: 121−127.

[24] ZHANG Peng, ZHANG Lin, WEI Dong-bin, WU Pei-fang, CAO Jing-wu, SHIJIA Cai-rang, QU Xuan-hui. A high-performance copper-based brake pad for high-speed railway trains and its surface substance evolution and wear mechanism at high temperature [J]. Wear, 2020, 444/445: 203182.

[25] XIAO Jin-kun, XIAO Shu-xian, CHEN Juan, ZHANG Chao. Wear mechanism of Cu-based brake pad for high-speed train braking at speed of 380 km/h [J]. Tribology International, 2020, 150: 106357.

[26] FANG Huan-chan, XIAO Peng, XIONG Xiang, YU Guang-jun. Microstructures, mechanical and oxidation behaviors of C/C composites modified by NiAl alloy [J]. Transactions of Nonferrous Metals Society of China, 2016, 26: 196−202.

[27] PENG Zheng, MIAO Chun-mao, SUN Wei, XU Yong-long, CHEN Hai-kun, LIU Yu-feng, ZHANG Hong-bo, XIONG Xiang. High-temperature thermal stability of C/C−ZrC−SiC composites via region labeling method [J]. Transactions of Nonferrous Metals Society of China, 2022, 32: 3349−3361.

[28] YANG Xin, HUANG Qi-zhong, ZOU Yan-hong, CHANG Xin, SU Zhe-an, ZHANG Ming-yu. XIE Zhi-yong. Anti-oxidation behavior of chemical vapor reaction SiC coatings on different carbon materials at high temperatures [J]. Transactions of Nonferrous Metals Society of China, 2009, 19: 1044−1050.

[29] SHAO Meng-meng, CHEN Zhao-ke, WANG Xin-shuang, WEN Qing-bo, XIONG Xiang. Ablation behavior and mechanisms of ZrC−SiC−$MoSi_2$ coated C/C−SiC−ZrC ceramic matrix composites under oxyacetylene torch [J]. Transactions of Nonferrous Metals Society of China, 2023, 33: 220−230.

[30] LI Yang, XIAO Peng, LI Zhuan, LUO Wei, ZHOU Wei. Oxidation behavior of C/C composites with SiC/$ZrSiO_4$−SiO_2 coating [J]. Transactions of Nonferrous Metals Society of China, 2017, 27: 397−405.

[31] AHMADIJOKANI F, SHOJAEI A, ARJMAND M, ALAYI Y, Yan Ning. Effect of short carbon fiber on thermal, mechanical and tribological behavior of phenolic-based brake friction materials [J]. Composites Part B−Engineering, 2019, 168: 98−105.

[32] JUSTIN ANTONYRAJ I, LENIN SINGARAVELU D. Tribological characterization of various solid lubricants based copper-free brake friction materials−A comprehensive study [J]. Materials Today: Proceedings, 2020, 27: 2650−2656.

[33] CONTESCU C I, AZAD S, MILLER D, LANCE M J, BAKER F S, BURCHELL T D. Practical aspects for characterizing air oxidation of graphite [J]. Journal of Nuclear Materials, 2008, 381: 15−24.

[34] LO I-HSUAN, YEH TSUNG-KUANG, PATTERSON E A, TZELEPI A. Comparison of oxidation behaviour of nuclear graphite grades at very high temperatures [J]. Journal of Nuclear Materials, 2020, 532: 152054.

[35] PAN T J, CHEN J, HE Y X, WEI W, HU J. Influence of grain refinement on oxidation behavior of two-phase Cu−Cr alloys at 973−1073 K in air [J]. High Temperature Materials and Processes, 2016, 35: 1005−1011.

[36] ZOU Lian-feng, LI J, ZAKHAROV D, STACH E A, ZHOU Guang-wen. In situ atomic-scale imaging of the metal/oxide interfacial transformation [J]. Nature Communications, 2017, 8: 307.

[37] LEITNER J, SEDMIDUBSKÝ D, JANKOVSKÝ O. The effect of nanosizing on the oxidation of partially oxidized copper nanoparticles [J]. Materials, 2020, 13: 2878.

[38] CUI Chun-juan, ZHANG Kai, WU Chong-yang, LAI Yuan-yuan, WANG Yan, SU Hai-jun. High temperature oxidation behavior of directionally solidified Fe(Al,Ta)/Fe_2Ta(Al) eutectic composite [J]. Journal of Alloys and Compounds, 2022, 913: 165210.

[39] YUAN Lu, WANG Yi-qian, MEMA R, ZHOU Guang-wen. Driving force and growth mechanism for spontaneous oxide nanowire formation during the thermal oxidation of metals [J]. Acta Materialia, 2011, 59: 2491−2500.

[40] XIANG Li-jun, GUO Jian, WU Chen-hui, CAI Meng-lei, ZHOU Xin-rong, ZHANG Nai-liang. A brief review on the

growth mechanism of CuO nanowires via thermal oxidation [J]. Journal of Materials Research, 2018, 33: 2264−2280.

[41] CAO Fan, JIA Shuang-feng, ZHENG He, ZHAO Lu-lu, LIU Hui-hui, LI Lei, ZHAO Li-gong, HU Yong-ming, GU Hao-shuang, WANG Jian-bo. Thermal-induced formation of domain structures in CuO nanomaterials [J]. Physical Review Materials, 2017, 1: 053401.

[42] FLAK D, CHEN Qian-li, MUN B S, LIU Zhi, RĘKAS M, BRAUN A. In situ ambient pressure XPS observation of surface chemistry and electronic structure of α-Fe_2O_3 and γ-Fe_2O_3 nanoparticles [J]. Applied Surface Science, 2018, 455: 1019−1028.

[43] XIAO Jin-kun, LI Tian-tian, CHEN Juan, ZHANG Chao. Effects of oxidation temperature on the microstructure and tribological performance of Cu-based brake pad for high-speed train [J]. Wear, 2023, 514/515: 204559.

高速列车铜基摩擦材料的氧化行为

肖金坤[1]，李天天[1]，鲍霆峰[1]，陈 娟[2]，张 超[1]

1. 扬州大学 机械工程学院，扬州 225127；
2. 扬州大学 测试中心，扬州 225009

摘 要：高速列车铜基摩擦材料在制动过程中，由于摩擦热的产生和耗散，会发生循环氧化。研究铜基摩擦材料在 300、400、500、600 和 700 ℃下等温氧化 50 h 的氧化行为。结果表明：铜基摩擦材料的氧化行为呈现多阶段特征；Cu、Fe 的氧化与氧的扩散共同控制着低温氧化过程，而石墨的氧化在 500 ℃之后占主导作用；Cu 的氧化首先形成 Cu_2O 纳米团簇，然后生成 CuO 纳米线，最后依次转变为细小的和粗大的等轴晶；氧化温度的升高会促进 Fe_2O_3 纳米片的生长和致密化；Cu 氧化物由于体积膨胀较大，逐渐将 Fe 氧化物覆盖；石墨烧蚀后形成的连通孔为内氧化提供氧气扩散通道；材料表面氧化层的形成使得表面硬度提高。

关键词：铜基摩擦材料；等温氧化动力学；氧化行为；表面形貌

(Edited by Bing YANG)